INFLUENCE OF LOADING HISTORY ON THE RESPONSE OF A REINFORCED CONCRETE BEAM

J.M. Ingham[1], D. Liddell[2] and B.J. Davidson[3]

ABSTRACT

An investigation considering the influence of loading histories on the performance of a reinforced concrete beam plastic hinge is described. Twelve loading histories were considered, including conventional procedures employed in the United States, Japan and New Zealand, and artificially generated histories derived from recorded earthquake ground motions. Details of the prototype structure and the test beam are described, followed by comprehensive reporting of experimental data. Performance descriptors and further treatment of the experimental data are presented in a companion paper.

1 INTRODUCTION

When a structure is subjected to an earthquake ground motion its response depends upon the attributes of the earthquake ground motion and the structure's dynamic and nonlinear characteristics, which includes hysteresis form and strength degradation properties. However, it is not possible to predict in advance the equivalent force-time history that a building may be subjected to because of the randomness inherent in the earthquake ground motion. To overcome this difficulty, researchers commonly adopt quasi-static cyclic loading histories of increasing amplitude and continue testing until the subassemblage suffers significant strength loss. This enables the likely seismic performance of structures and their components to be determined. Parameters such as the curvature ductility capacity of plastic hinges and the influence of joint and member shear deformations are calculated from test data, from which the available structural capacity of subassemblies and structural forms is derived. To establish whether acceptable capacity is achieved, these conclusions need to be compared with the predicted demand corresponding to a design level earthquake.

Presently researchers are showing considerable interest in displacement-based methods of structural design, proposing that these methods lead to more rational, safer, and cost-effective designs. For these reasons it has been suggested that these methods be introduced in combination with the next release of the New Zealand Loadings Code. One of the key attributes of designing structures using displacement-based methods is the selection of a target ultimate displacement. This decision is based on the performance of laboratory subassemblies. However, the simulated loading history applied to subassemblies in the laboratory will be different from that arising when the structure is shaken during an earthquake. Hence the influence which the laboratory load history has on the resultant conclusions warrants careful consideration.

Compounding this issue is that the applied loading history often varies between research institutions throughout the world. It is desirable to be able to compare experimental results from testing using different loading histories, and also compare the demands placed on a structure or structural component from these different tests with the demands generated by a design level earthquake. In this study twelve nominally-identical reinforced concrete beams were subjected to a variety of different loading histories to ascertain the influence of loading history on the measured response.

2 TEST ASSEMBLY DESIGN, CONSTRUCTION, AND SET-UP

The Cement and Concrete Association of New Zealand (CCANZ) has published a guide (CCANZ 1998) demonstrating the design of a ten-storey office building to the requirements of the New Zealand Standard for the Design of Concrete Structures (Standards New Zealand 1995). This guide is commonly known, and hereafter referred to, as 'The Red Book'. The example presented in the Red Book provided the prototype design for this project, and was chosen due to its high profile among New Zealand structural engineers.

[1] *Cement and Concrete Association Lecturer, Department of Civil and Resource Engineering, University of Auckland, Auckland (Member)*

[2] *Design Engineer, Connell Wagner Ltd, Auckland (Member)*

[3] *Department of Civil and Resource Engineering, University of Auckland, Auckland (Fellow)*

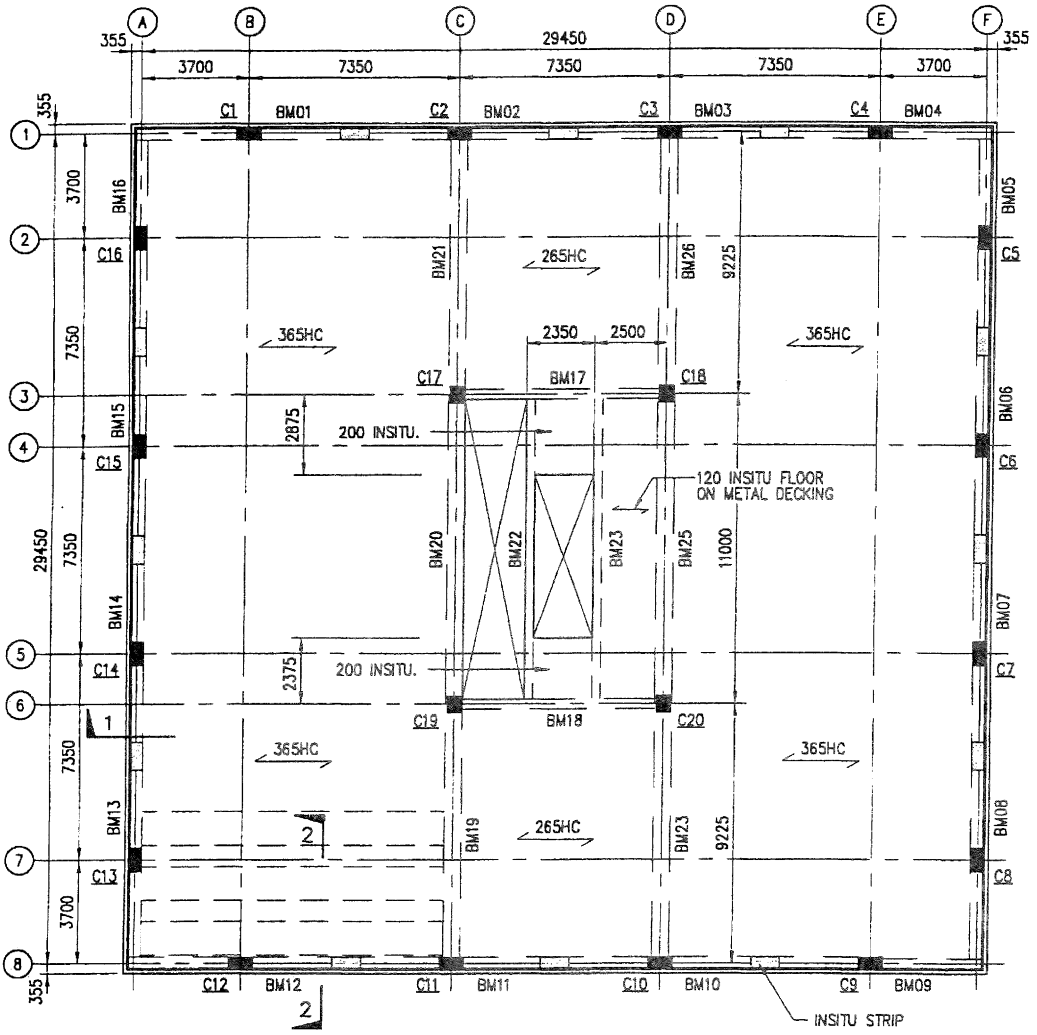

Figure 1 Frame Building Plan (CCANZ 1998).

A reinforced concrete frame was chosen because buildings are much more prevalent in New Zealand than other structural forms, such as bridges, and the majority of these buildings are comprised of reinforced concrete.

2.1 Prototype Design

Fig. 1 illustrates the location of the internal and perimeter frames of the prototype office building and Fig. 2 presents an elevation of the perimeter frame. Grid F was the critical frame, as frames on the alphabetical grids had larger gravity loading than frames on the number grids due to the orientation of the precast hollow core flooring slabs. Fig. 3 displays the output from the combined modal analysis including P-Δ effects for the perimeter frame located on Grid F, indicating that Level 2 was the critical design level.

To simulate the response of a beam section under seismic loading it was necessary to base the design of the test assembly on a beam dominated by seismic loading. The beams where seismic loads were most dominant were those perimeter beams running parallel with the orientation of the floor slabs. Fig. 1 demonstrates that beams along Grids 1 and 8 fulfilled this criterion.

Fig. 4 presents the reinforcement layout for the reinforced concrete frame along Grid 8 at Level 2. Detailing of the test assembly was based on the central beam where the longitudinal reinforcement consisted of 4-HD24 top and bottom. Fig. 5 details a cross section of the prototype beam taken through the plastic hinge zone.

2.2 Test Set-Up

Testing of twelve 2/3rd-scale beams reported herein was conducted using the set-up presented in Figs. 6 and 7. Fig. 6 indicates that the test set-up consisted of two separate beams placed symmetrically on a concrete pedestal. The test assembly was stressed to the strong floor with six stressing rods as demonstrated in Fig. 7. This ensured that structural deformations were not primarily attributable to rigid body rotation of the beam on its pedestal.

Fig. 6 illustrates that the beam on the opposite side of the pedestal to the actuator was left unsupported. This was to minimise the transfer of forces and strains from the first beam into the second beam during testing. A steel brace was placed on the end of the first beam to prevent torsional response. A 200 mm high concrete appendage was placed on

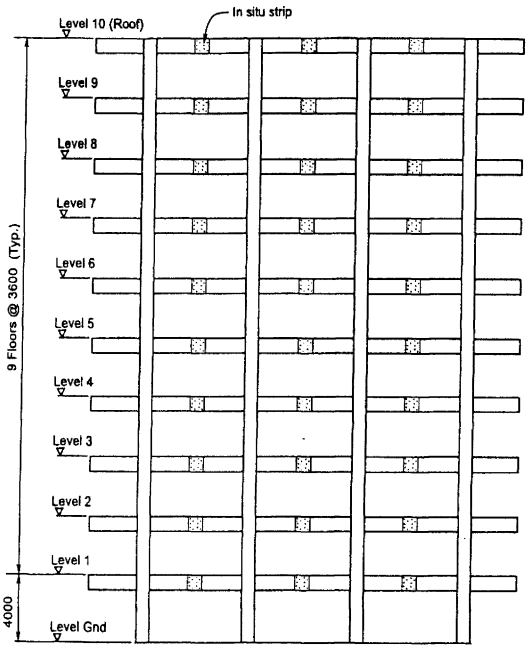

Figure 2 Perimeter Frame Elevation (CCANZ 1998).

top of the beam in the joint region to ensure that a uniform stress was applied to the joint region from the stressing rods.

An actuator was placed 2.15 m from the pedestal face to simulate the response of the prototype, when subjected to seismic loading. This distance was based on half the clear distance between columns on Grids 1 and 8 in Fig. 1, multiplied by a 2/3rd scale factor.

2.3 Test Unit Details

Laboratory restraints required the prototype design to be reconstructed at 2/3rd scale. The resultant reinforcement details are illustrated in Figs. 8 and 9. Fig. 9(a) details the longitudinal and transverse reinforcement through the plastic hinge zone (Section A-A), and Fig. 9(b) details the longitudinal and transverse reinforcement outside the plastic hinge zone (Section B-B).

The joint design of the test unit was modified from the example presented in the Red Book so that testing of the first beam did not affect the second beam of each assemblage. An extra reinforcing bar was welded to each longitudinal bar in the joint region, and the length of the beam-column joint was

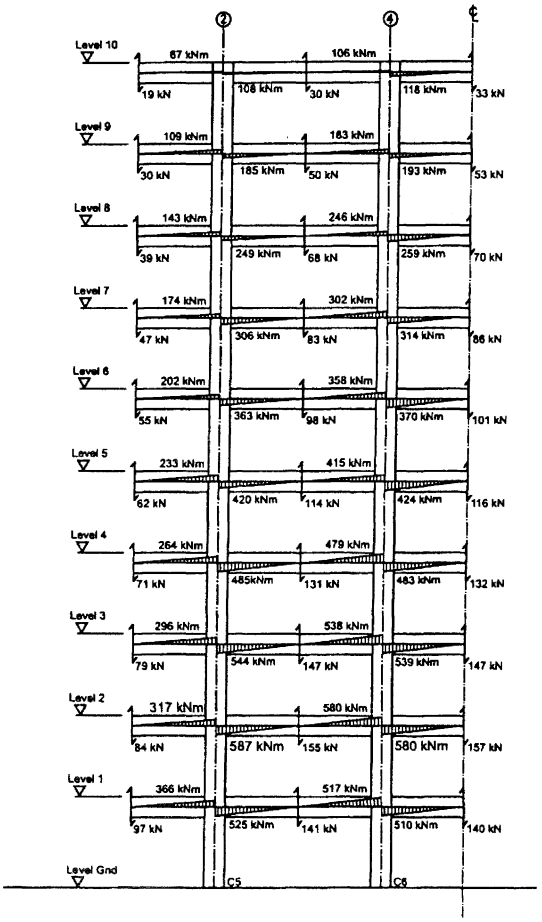

Figure 3 Frame design Actions (CCANZ 1998).

increased. This allowed a greater amount of vertical reinforcement in the joint region than the scaled amount from the prototype design. Fig. 10 illustrates the modifications made to the joint region of the test unit.

2.4 Material Properties

The concrete mix had a specified 28-day strength of 30 MPa and specified slump of 100 mm, with a measured average 28-day strength of 38.4 MPa. To eliminate differences in concrete strength due to different production batches, the concrete for all twelve beams was placed in a single pour (see Fig. 11). The concrete was cured for a period of 80 days instead of the standard 28 days. The history of the concrete

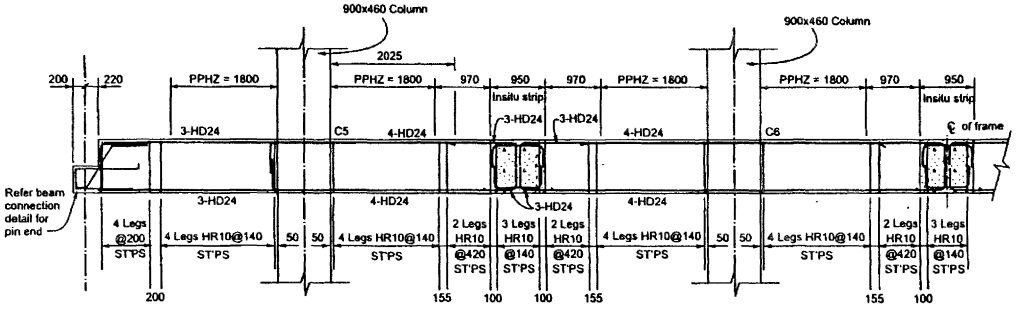

Figure 4 Level Two Reinforcement Layout (CCANZ 1998).

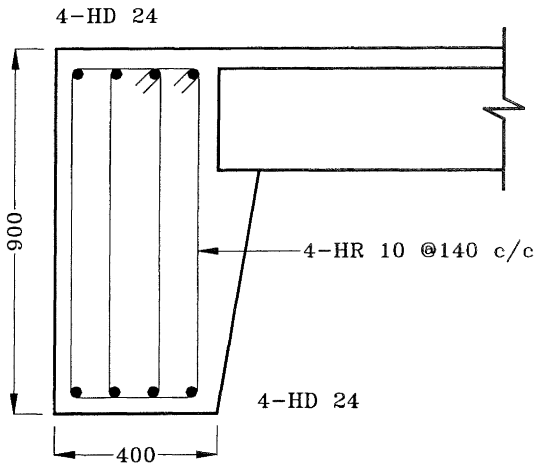

Figure 5 Prototype Cross Section (CCANZ 1998).

strength over time, illustrated in Fig. 12, demonstrates that the concrete had gained the majority of its strength after 80 days.

Differences in reinforcement material properties were minimised by obtaining the reinforcing steel for all twelve beams from the same production batch. Fig. 13 presents stress-strain curves from four randomly selected longitudinal reinforcement samples. The average yield strength and Young's modulus was 467 MPa and 197 GPa respectively.

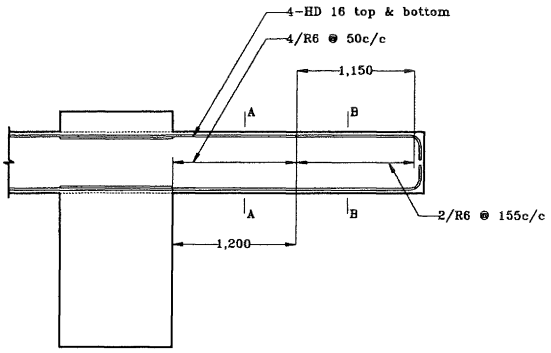

Figure 8 Reinforcement Layout in Test Sub-Assemblage.

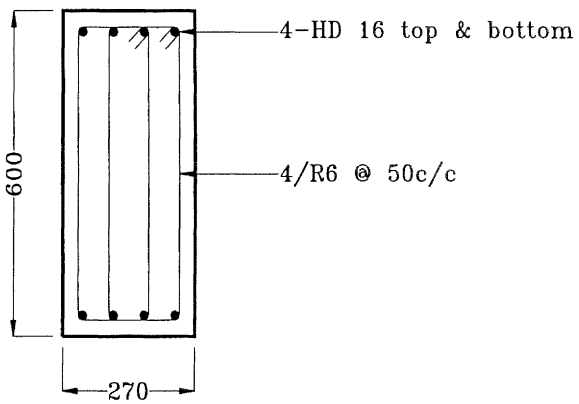

Figure 9(a) Cross Section at A-A (see Fig. 8).

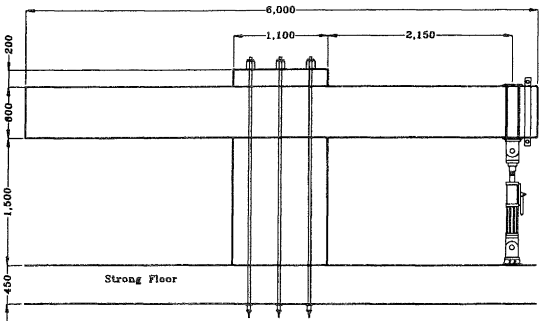

Figure 6 Front Elevation of Test Set-Up.

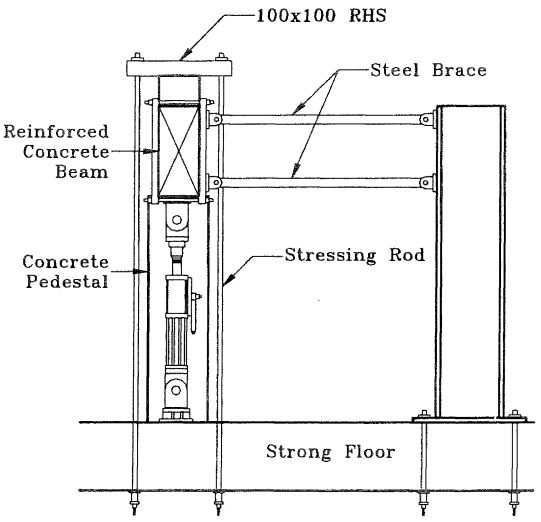

Figure 7 End Elevation of Test Set-Up.

2.5 Instrumentation

During fabrication of the reinforcement cage, steel studs were welded onto the longitudinal reinforcement at positions shown in Fig. 14. Displacement transducers were connected to these studs to measure relative displacements between the studs during testing. This enabled the calculation of longitudinal reinforcement strains as well as flexural, shear, and rocking components of displacement for various loading stages. Beam vertical displacements were measured using a linear potentiometer at the position of the vertical actuator,

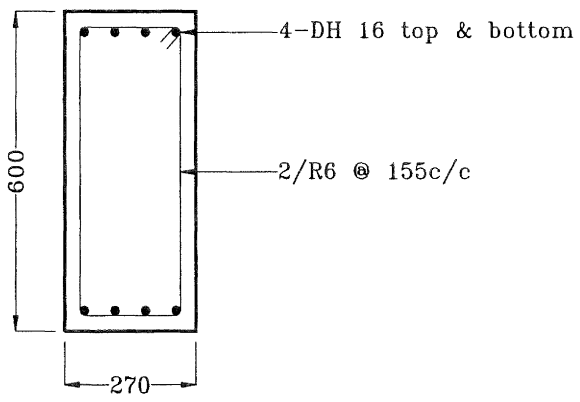

Figure 9(b) Cross Section at B-B (see Fig. 8).

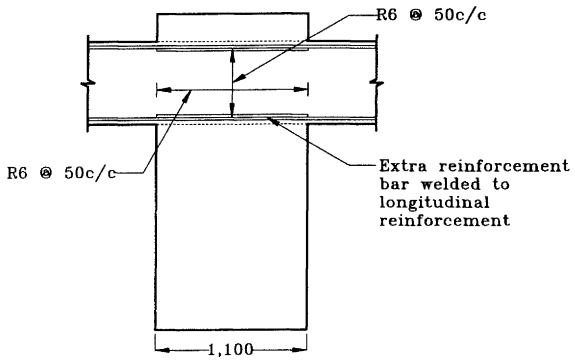

Figure 10 Beam Column Joint.

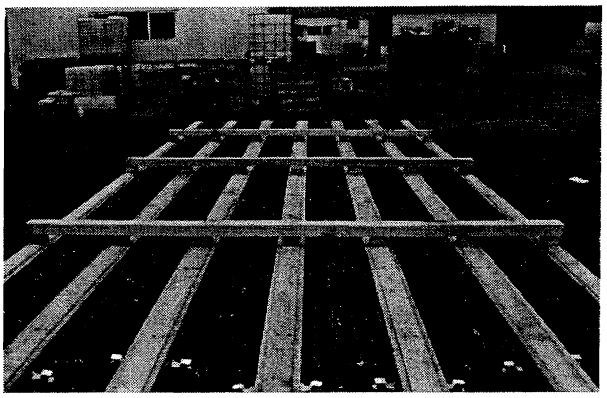

Figure 11 Reinforcement Cages Positioned in Boxing.

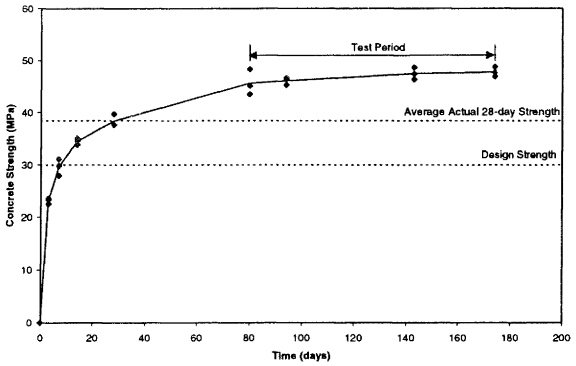

Figure 12 History of Concrete Strength.

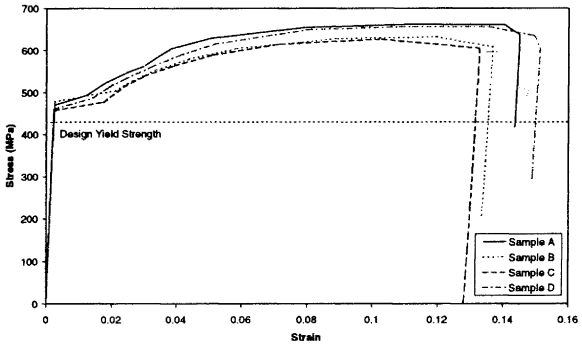

Figure 13 Stress-Strain Curve for Longitudinal Reinforcement.

and the magnitude of the vertical force was determined using the actuator load cell.

2.6 Nominal and Ideal Design Strengths

Nominal design strengths were based on specified materials properties, with the increase in concrete strength over time and higher than specified material strengths being ignored. The nominal design strengths were denoted with a subscript 'n'. Ideal design strengths accounted for the increase in concrete strength over time and the higher than specified material strengths. However, an ultimate concrete compressive strain of 0.003 and a rectangular stress block were still assumed. As for nominal design strength calculations, strain hardening in the longitudinal reinforcement and confinement effects from the transverse reinforcement were ignored. The ideal design strengths were denoted with a subscript 'i'.

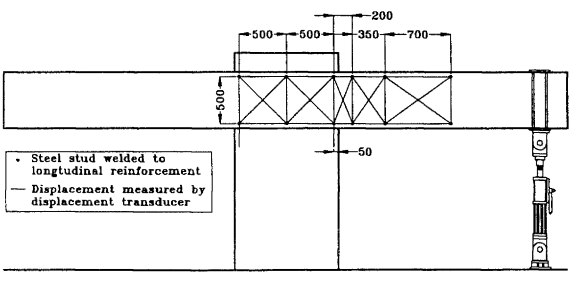

Figure 14 Instrumentation Layout.

2.7 Sign Conventions

The positive direction of loading referred to the upper right quadrant of the measured hysteresis response, a push force in the actuator, and tension on the lower edge of the beam (see Fig. 15).

3 APPLIED LOADING HISTORIES

Twelve different loading histories were applied to twelve nominally-identical reinforced concrete beams. To facilitate effective performance comparison, a common definition of failure was required. The control for the testing reported herein was the New Zealand loading history. The other eleven loading histories consisted of three loading histories commonly applied in research institutions in the United

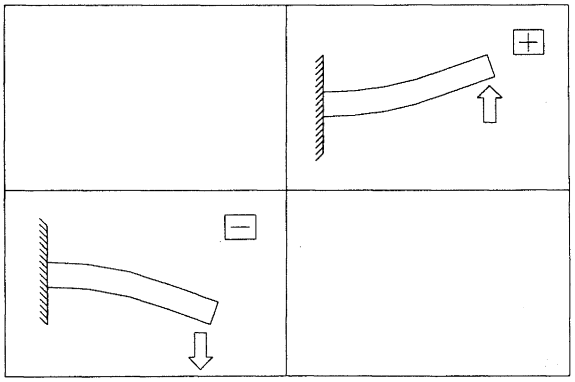

Figure 15 Sign Convention.

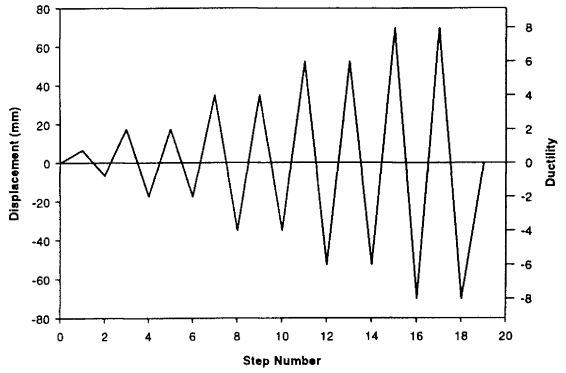

Figure 16(a) New Zealand Loading History.

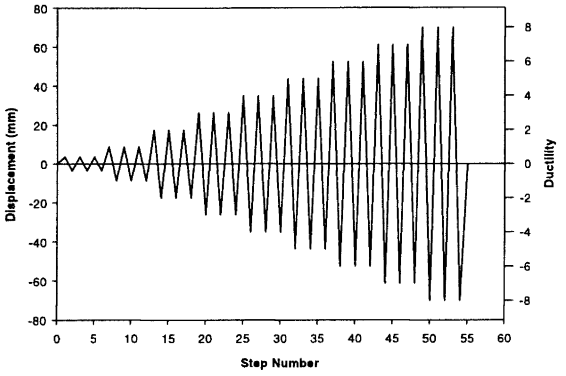

Figure 16(b) Loading History Applied at the University of California at Berkeley.

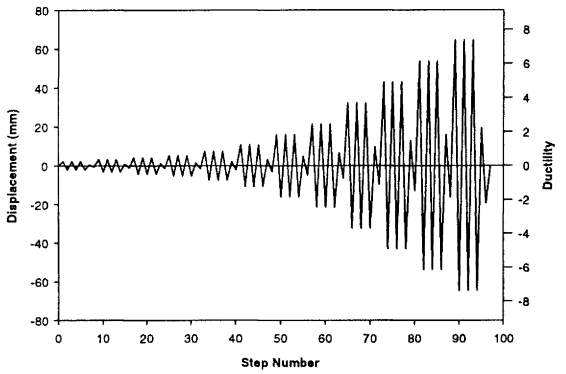

Figure 16(c) PRESSS Loading History.

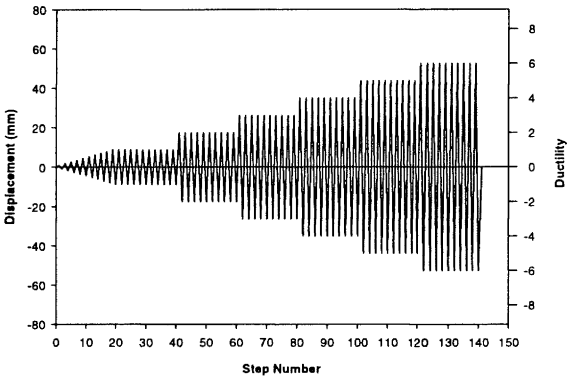

Figure 16(d) Public Works Research Institute Loading History.

States and Japan, three fabricated histories, and five simulated responses from the ten-storey building subjected to different acceleration sequences.

3.1 New Zealand Loading History

The control for this series of experiments was the conventional New Zealand loading history (Park 1989). This procedure is presented schematically in Fig. 16(a). A yield displacement equal to 8.75 mm was established using this procedure.

3.2 Comparison with International Procedures

Three test assemblies were subjected to conventional loading histories from the United States and Japan so that experimental results from those countries could be compared with results obtained using the New Zealand loading history. The chosen research institution from the United States was the University of California at Berkeley (UCB). It should be noted that the loading history applied at UCB was similar to loading histories applied at other US universities. Hence the loading history applied at UCB was taken to be indicative of general practice in universities located on the West Coast of the United States. Fig. 16(b) illustrates the conventional approach from UCB. A literature review of testing procedures applied at UCB found minor variation of the adopted procedure. This project followed the approach reported by Ma et al. (1976), where three cycles were applied at each ductility level.

The PRESSS research programme involved a large number of research institutions throughout the United States (Ingham 2000) and the load history from that programme was applied in this study due to this wide coverage. The loading history adopted for the PRESSS research programme (Stone et al. 1995) was based on storey drifts, which were converted to ductility levels in this study to assist in the comparison of experimental results. The initial drift level was 0.1% and the drift level increased in increments of 0.05% until 0.25%. The drift level was then increased in increments of 0.1%, 0.15%, and two increments of 0.25%. After these cycles, the drift level was increased in increments of 0.5% until failure occured. As shown in Fig. 16(c), three cycles were completed at each drift level, followed by an intermediate elastic cycle. In the elastic cycle, the test unit was loaded to 30 percent of the peak load in the preceding three cycles.

Fig. 16(d) illustrates the procedure adopted by the Public Works Research Institute (PWRI). The force-controlled component consisted of several increasing force cycles up to the calculated yield force. The initial force was 10% of the calculated yield force with the force then being increased in increments of 10% of the yield force until the yield force was reached.

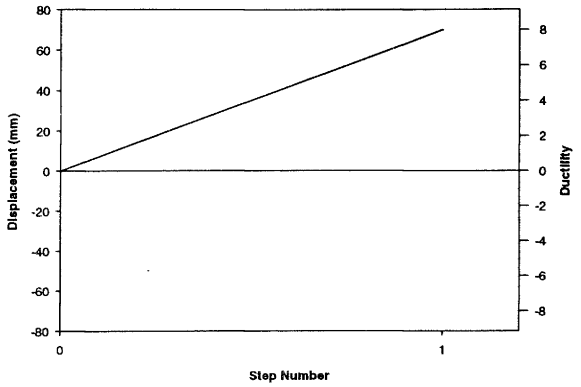

Figure 17(a) Monotonic Loading History.

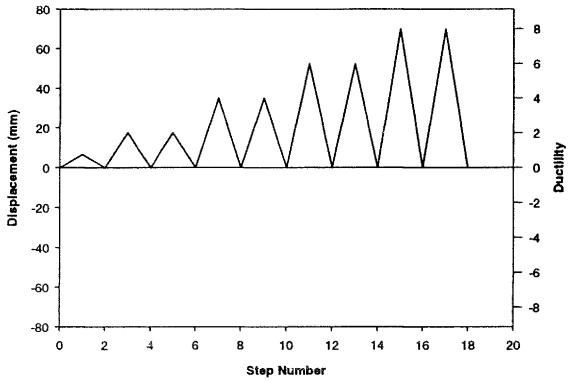

Figure 17(c) Unidirectional Cycling History.

Once the force-controlled component had been completed, loading was controlled by selected tip displacements that increased in single ductility increments. The number of cycles to each ductility step varies according to the member and ground motion characteristics. One cycle at each ductility step is applied if the member is not affected by the load history. Three cycles are applied if the ground motion is an inter-plate earthquake, whereas ten cycles are applied if the ground motion is from a large plate-boundary earthquake. Ten cycles were applied at each ductility level in this study.

3.3 Fabricated Loading Histories

The three fabricated loading histories applied in this study were monotonic loading, bi-directional cycling at ductility 8, and unidirectional cycling. One of the test subassemblies was subjected to monotonic loading, as presented in Fig. 17(a), to establish the skeleton force-displacement response of the test subassemblage. Bi-directional cycling at ductility 8, as illustrated in Fig. 17(b), was conducted to give an indication of the fatigue characteristics of the test subassemblage. The third fabricated loading history consisted of the New Zealand loading history applied to a test subassemblage in a single direction, so that a comparison could be made between results from reversed cyclic loading and uni-directional cyclic loading. This is illustrated in Fig. 17(c).

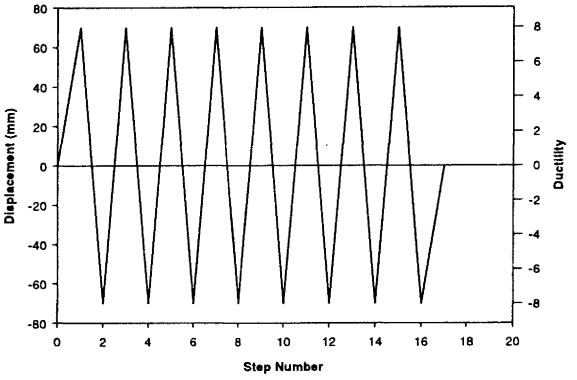

Figure 17(b) Direct Cycling at Ductility 8.

3.4 Simulated Response of the Ten-Storey Building

One of the objectives of this study was to determine whether the order of earthquake records within an acceleration history affects the experimental results. In Ingham et al. (2001), the procedure followed to simulate the seismic response of the ten-storey building is discussed. Five acceleration histories consisting of four or five scaled earthquake records were developed. All five sequences were applied under displacement control and in each case, the entire loading sequence was completed regardless of subassemblage degradation. These loading histories are illustrated in Fig. 18.

4 ANALYSIS OF RESULTS

A significant amount of data was obtained from the twelve tests. This section compares the overall force-displacement response, the response from each test for various ductility levels, the composition of measured deformations, the energy dissipation characteristics, measured beam elongation, and the strain behaviour of the reinforcement steel. The measured crack behaviour from the seven laboratory procedures is also discussed.

4.1 Displacement Ductility Capacity

4.1.1 Laboratory Procedures

Fig. 19(a) presents the force-displacement response from testing using the New Zealand loading history and reveals that the beam reached a maximum ductility of 10. Fig. 19(b) illustrates that an ultimate ductility of 10 was also reached when the UCB loading history was applied. Fig. 19(c) presents the force-displacement response for the PRESSS loading regime. The beam reached an ultimate ductility of 8.6 in the positive direction and 7.4 in the negative direction, with strength then gradually decreasing over a number of cycles. Fig. 19(d) displays the force-displacement response from testing using the PWRI loading history. Strength dropped to below 80% of the maximum-recorded on the third cycle at ductility 6 in the positive direction and on the fifth cycle at ductility 6 in the negative direction.

Fig. 20(a) illustrates the force-displacement response for the monotonic loading history. The maximum stroke of the actuator was reached after the test subassemblage was loaded to ductility 22. However, the strength of the test specimen

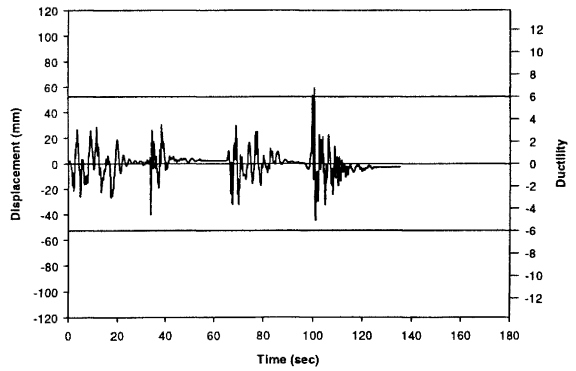

Figure 18(a) Critical Beam Displacement-Time History (Acceleration History A).

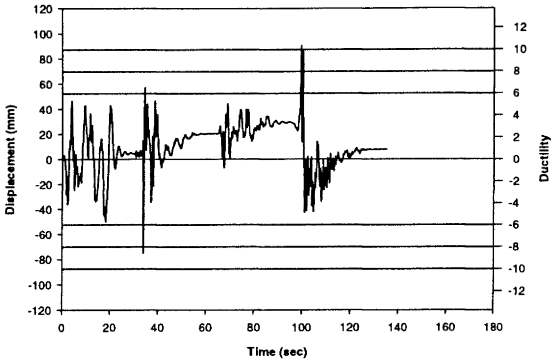

Figure 18(b) Critical Beam Displacement Time History (Acceleration History B).

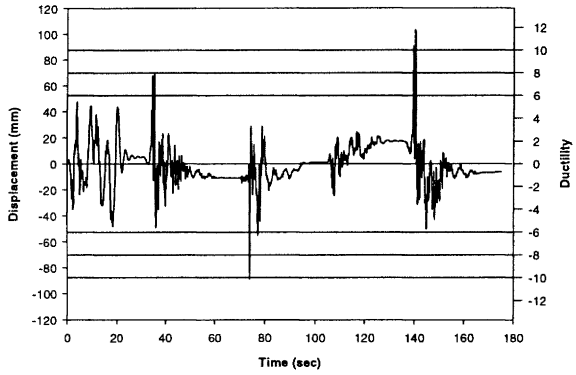

Figure 18(c) Critical Beam Displacement Time History (Acceleration History C).

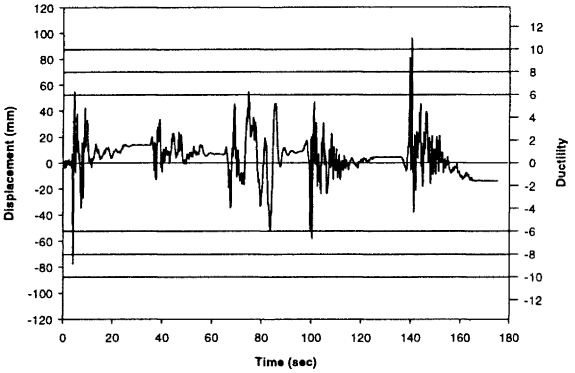

Figure 18(d) Critical Beam Displacement Time History (Acceleration History D).

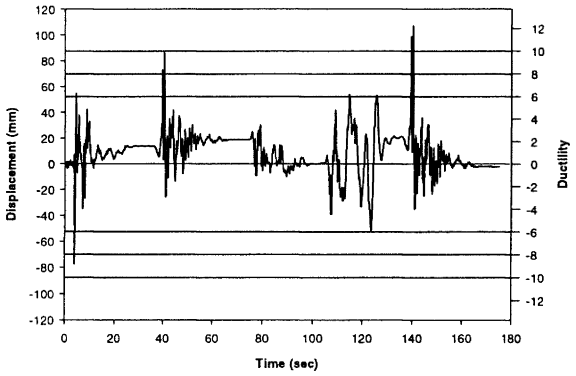

Figure 18(e) Critical Beam Displacement Time History (Acceleration History E).

had begun to reduce and extrapolation of the force-displacement response gave an ultimate ductility of 23. This is far in excess of the maximum displacement obtained from the New Zealand loading history and was directly attributable to the monotonic loading regime.

Fig. 20(b) presents the force-displacement response from testing that applied bi-directional cycling at ductility 8. Five complete cycles at ductility 8 were applied before the strength of the test specimen dropped below 80% of the maximum-recorded strength for that test. Fig. 20(c) reveals that the test assemblage reached an ultimate ductility of 22 under unidirectional loading before failure occurred. Failure was attributed to low-cycle fatigue of the reinforcing steel.

The seven force-displacement plots presented in Figs. 19 and 20 reveal large discrepancies between the ultimate displacement established from testing using the seven laboratory procedures. Firstly, the ultimate displacement of the test specimen subjected to monotonic loading was far in excess of the ultimate displacement of the test specimens subjected to any of the five bi-directional cyclic procedures. More critically, the ultimate displacement derived from loading histories applied at different research institutions also varied. Testing conducted using the PWRI loading history was the most conservative and returned an ultimate ductility of 6. In contrast, an ultimate ductility equal to 10 was established from testing where the New Zealand and UCB loading histories were applied. Of the two, the New Zealand loading history was taken to be the least conservative. Testing using the PRESSS loading regime returned an ultimate ductility of 7.4, which is between the bounds previously reported.

The above results suggest that structures designed in Japan using displacement-based methods would be designed more conservatively than the corresponding structure in New Zealand or the United States.

Failure was not necessarily measured when testing using the five acceleration histories (see Fig. 21). For acceleration

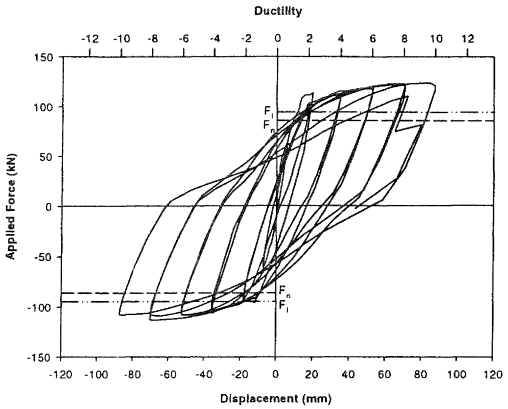

Figure 19(a) Force-Displacement Response (New Zealand Loading History).

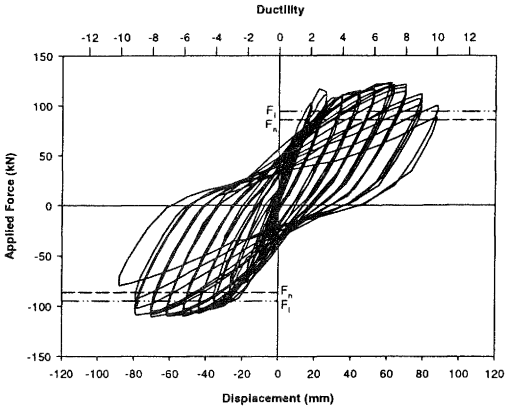

Figure 19(b) Force-Displacement Response (UCB Loading History).

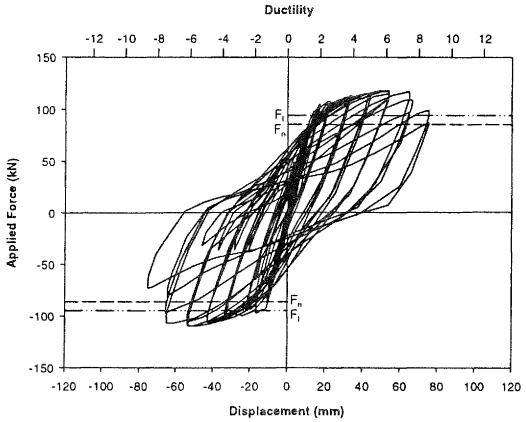

Figure 19(c) Force-Displacement Response (PRESSS Loading History).

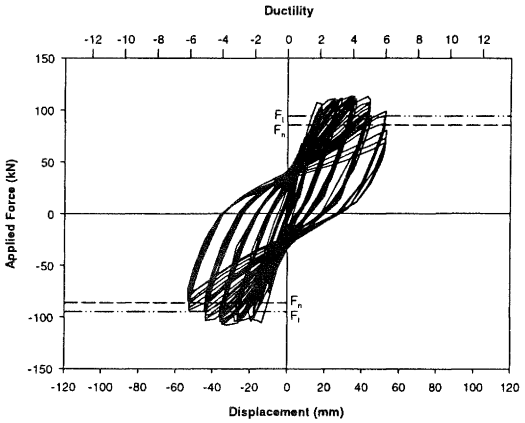

Figure 19(d) Force-Displacement Response (Public Works Research Institute Loading History).

history A, this was due to scaling issues (refer to Ingham et al. 2001). For the remaining acceleration histories it proved difficult to identify failure as defined by the onset of significant strength degradation. This was because the largest ductility cycles often did not require the application of a large force due to their position in the displacement sequence. Thus, it was difficult to determine whether any strength loss was due to the degradation of the test specimen or the position of the cycle in the displacement sequence.

The loading sequence from acceleration history D was the only loading sequence that definitely resulted in failure of the test unit. Fig. 21(d) reveals that significant strength degradation occurred during the test, but failure was attributed to the influence of welded instrumentation studs, resulting in premature failure of the longitudinal reinforcement.

Failure of the other test subassemblages had still not occurred after being subjected to four earthquake records, even though all four records were scaled up by various factors and two records were from severe earthquakes. On the evidence of the testing reported herein, it is proposed that structures designed using force-based methods have a large degree of conservatism inherent in their design. This has also been noted by Priestley (1997) in his work on displacement-based methods of structural design.

4.2 Comparison of Force-Displacement Hysteresis Loops

Fig. 22(a) compares the force-displacement hysteresis loops from six of the seven laboratory procedures after the first cycle at ductility 4. Response from testing using the PWRI loading history and the UCB loading history showed more pinching of the hysteresis loops than the response from testing using the New Zealand loading history. The highest reloading stiffness was from unidirectional testing whereas the lowest was from testing using the PWRI and UCB loading histories. Fig. 22(a) reveals that the post-yield force-displacement response from monotonic loading formed an envelope to the corresponding phase of the force–displacement response from the cyclic tests.

Fig. 22(b) compares the force-displacement hysteresis loops from six of the seven laboratory procedures after the first cycle at ductility 6. The response from testing using the PWRI loading history shows considerably more pinching and a lower reloading stiffness than the response from other cyclic tests.

Fig. 22(c) contrasts the force-displacement hysteresis loops from six of the seven laboratory procedures after the first cycle at ductility 8. The response from testing using bi-directional cycling at ductility 8 showed considerably less

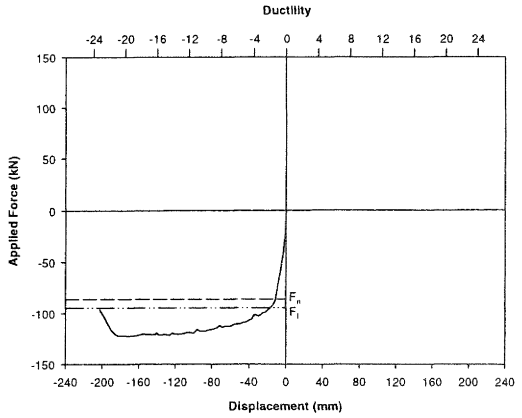

Figure 20(a) Force-Displacement Response (Monotonic Loading).

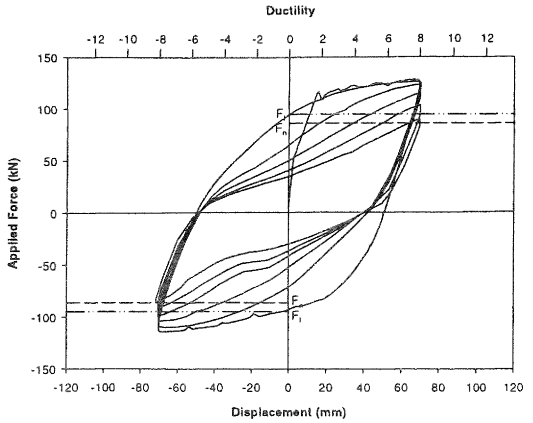

Figure 20(b) Force-Displacement Response (Cycling at Ductility 8).

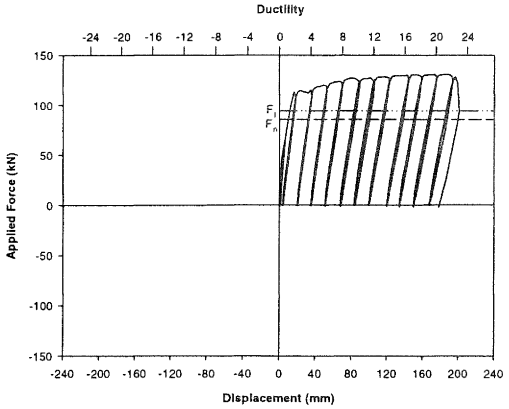

Figure 20(c) Force-Displacement Response (Unidirectional Loading).

pinching and a significantly higher reloading stiffness than response from the other cyclic tests.

It was established from Figs. 22(a)-(c) that the response from testing using the New Zealand loading history was not reflective of the response from testing using other laboratory procedures due to the larger ductility increments that were applied as part of the New Zealand loading history. These figures also indicate that response from testing using the PWRI loading history was not reflective of the response obtained using either of the two loading histories from research institutions in the United States, presumably because of the larger number of cycles that were applied at each ductility level.

Fig. 22(d) compares the force-displacement envelopes from the five acceleration histories with the response from monotonic loading. The influence of the largest displacement cycles' position in the displacement sequence on the shape of the hysteresis loops is illustrated. The maximum negative displacement for acceleration histories D and E was at the beginning of the first earthquake record whereas the maximum negative displacement for acceleration histories B and C was during the second and third earthquake records respectively. This was reflected in the greater amount of pinching in the hysteresis loops for acceleration histories B and C because of the degradation that had occurred prior to the application of the maximum displacements in the negative direction. The amount of pinching in the hysteresis loops after application of the maximum displacement in the positive direction was comparable for each acceleration history because these displacements were in each case applied near conclusion of the test. However, even though variations in hysteretic behaviour occurred, comparable degradation at the conclusion of acceleration histories B, C, and E was observed.

4.3 Composition of deformation

From the instrumentation layout detailed in Fig. 14 it was possible to determine the magnitude of deformation that was attributable to the three components: rocking of the beam on its pedestal; vertical beam-end displacements due to shear deformations; and vertical beam-end displacements due to flexural deformations. The composition of deformations is shown in Fig. 23 for the laboratory procedures and fabricated loading histories and in Fig. 24 for the acceleration histories.

From Figs. 23 and 24 it may be determined that in general there was good correlation between the sum of the calculated components of deformation and the measured total vertical displacement. In all cases the predominant mode of deformation was flexure, and rocking of the beam on its support was of limited significance. In general Figs. 23(a)-(d) and Fig. 24 indicate that shear deformations became increasingly predominant at larger vertical displacements. Fig. 23(a) indicates that flexural deformations were more predominant when using the New Zealand loading history than when using the other laboratory procedures. This is consistent with the data shown in Fig. 22, where the hysteresis response was less pinched for the New Zealand history than for the other laboratory procedures.

Figs. 23(e)-(g) suggest that shear deformations were least prevalent in the fabricated loading histories, but that in general all the laboratory procedures had shear deformations of a similar character to those generated when testing using the acceleration histories.

4.4 Energy Dissipation

The amount of energy dissipated during each test was calculated so that energy characteristics could be compared.

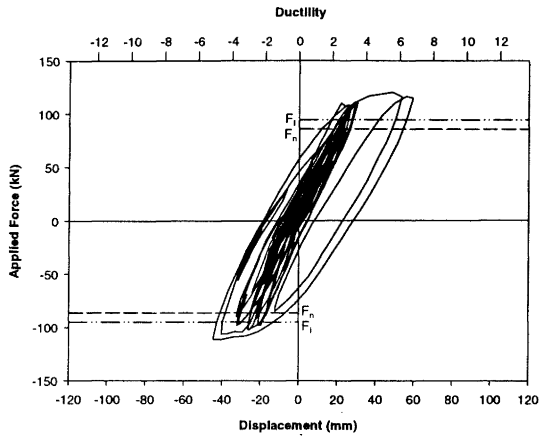

Figure 21(a) Force-Displacement Response (Acceleration History A).

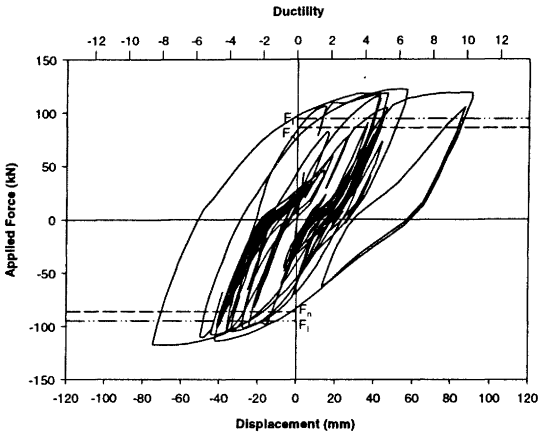

Figure 21(b) Force-Displacement Response (Acceleration History B).

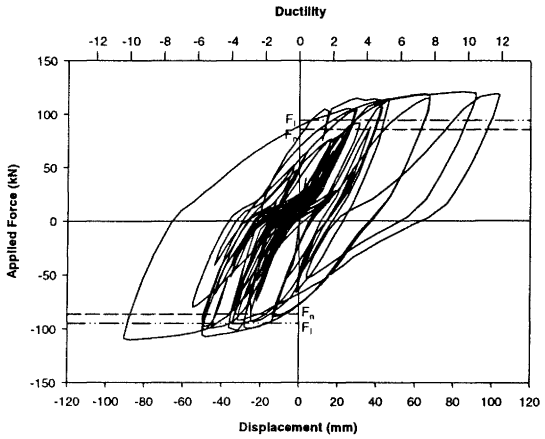

Figure 21(c) Force-Displacement Response (Acceleration History C).

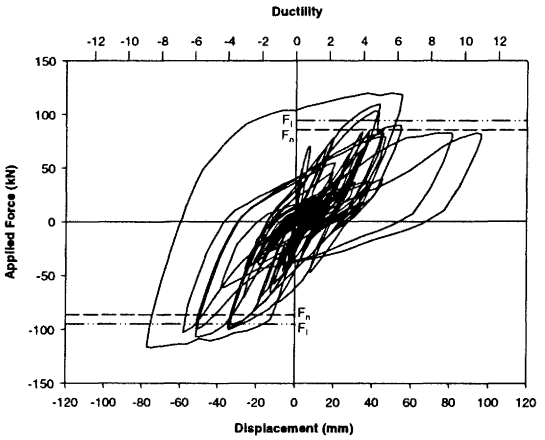

Figure 21(d) Force-Displacement Response (Acceleration History D).

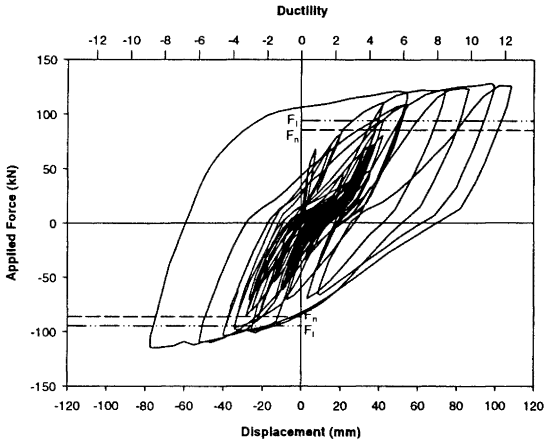

Figure 21(e) Force-Displacement Response (Acceleration History E).

The amount of energy dissipated during the test was defined as the area inside the hysteresis loops until failure occurred. Fig. 25 indicates that the energy dissipation characteristics were strongly load history dependent.

Fig. 25(a) reveals significant differences between the energy dissipated during testing using the four loading histories from research institutions, with little consistency in either the cumulative dissipated energy or the measured cumulative ductility.

Fig. 25(b) compares the energy dissipation characteristics from testing using the five acceleration histories and demonstrates that the characteristics from acceleration histories B–E were similar. Fig. 25(b) demonstrates that a lower amount of energy was dissipated during testing using acceleration history D than acceleration histories C and E, even though an identical number of earthquake records were applied. This was due to the premature failure that occurred when testing using acceleration history D.

4.5 Horizontal beam elongation

Horizontal beam elongation is generated when reinforcement is plastically strained in tension during plastic hinge formation. If this reinforcement is not equally plastically strained in compression during the reversing load cycle, then cracks remain open and the beam elongates.

Beam elongation histories are reported in Fig. 26 for the laboratory procedures and fabricated loading histories, and in Fig. 27 for the acceleration histories. This data indicates that there was considerable variation in the measured magnitude

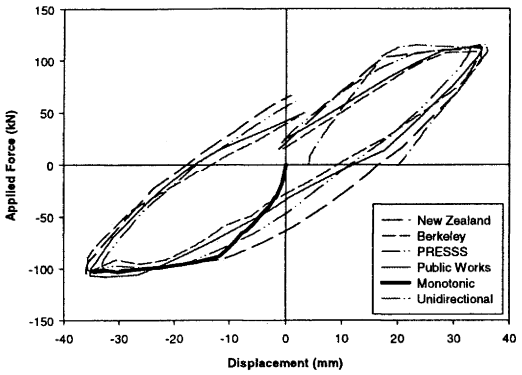

Figure 22(a) Comparison after Loading to Ductility 4.

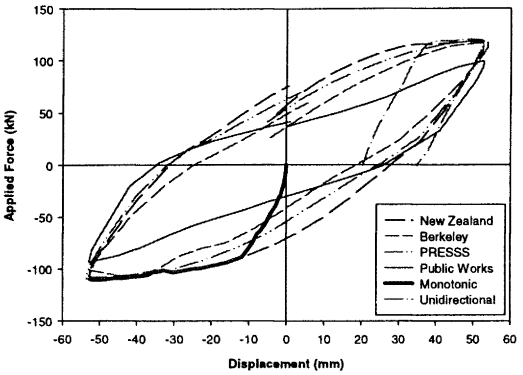

Figure 22(b) Comparison after Loading to Ductility 6.

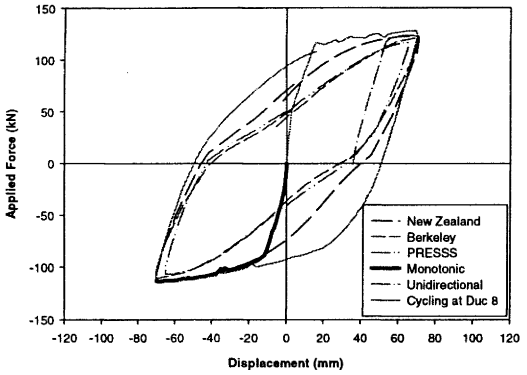

Figure 22(c) Comparison after Loading to Ductility 8.

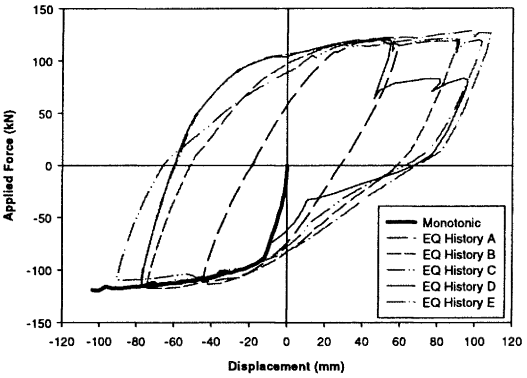

Figure 22(d) Comparison of Acceleration Histories' Envelope with Monotonic Response.

of beam deformation. Partly this can be correlated with the magnitude of plastic rotations, as indicated in Fig. 26(d) where the PWRI loading history resulted in failure at a smaller magnitude of vertical displacement, and similarly generated reduced beam elongation.

Fig. 27 indicates that beam elongation resulting from the acceleration records was in most cases of a larger magnitude than that arising from laboratory test procedures, with UCB and PRESSS loading histories resulting in the closest correlation. In general, beam elongation generated from the acceleration loading histories was of the order of 5-6% of the beam depth.

4.6 Reinforcement Steel Strain Behaviour

Fig. 28(a) presents the reinforcement strain envelopes from the seven laboratory procedures for loading up to and including ductility 8, when the instrumentation devices were removed. This figure reveals that, apart from bi-directional cycling at ductility 8, response was generally symmetric. Fig. 28(a) also demonstrates that similar strain readings were recorded from monotonic and unidirectional loading.

Fig. 28(b) displays the reinforcement strain envelopes from testing using the five acceleration histories, with non-symmetric response due to the irregular displacement sequences applied. Strain accumulation behaviour was most comparable to the response from testing using bi-directional loading at ductility 8.

The largest strains from the seven laboratory procedures were recorded during testing using the New Zealand loading history. This and the comparison made regarding energy dissipation indicates that the New Zealand loading history replicated the earthquake demand more closely than loading histories from other research institutions.

4.7 Comparison of Crack Behaviour

This section details the width of the predominant cracks that resulted from testing using the seven laboratory procedures. Comparisons were made at the conclusion of the cycles at ductility 2, ductility 4, and ductility 6. No comparisons were made between the crack behaviour from testing using the five acceleration histories because of their irregular nature.

Little cracking occurred outside the instrumentation zone for any of the tests, with none of the cracking from outside the instrumentation zone being open significantly at any stage of any test. This indicated that the instrumentation layout depicted in Fig. 14 recorded all the necessary data.

4.7.1 Comparison after Loading to Ductility 2

Table 1 compares the widths of the two major cracks in the plastic hinge zone at ductility 2, with the letters 'A' and 'B'

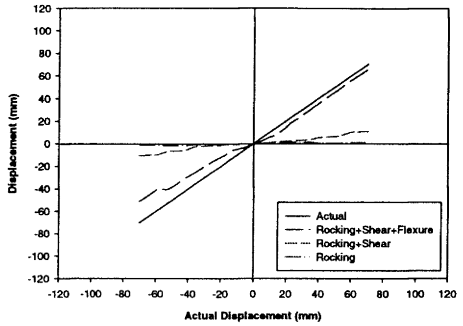

Figure 23(a) Components of Displacement (New Zealand Loading History).

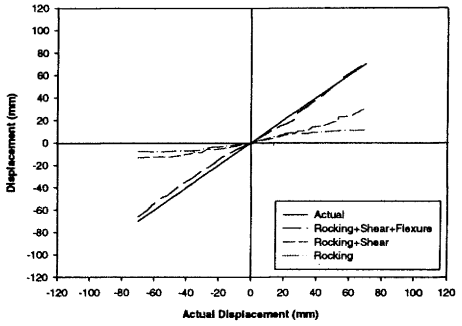

Figure 23(b) Components of Displacement (UCB Loading History).

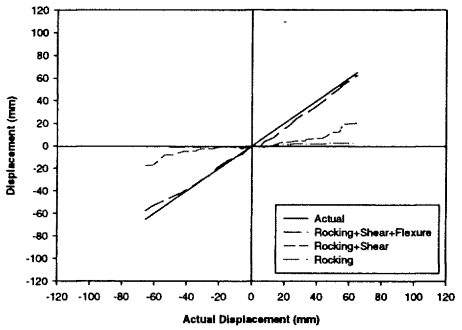

Figure 23(c) Components of Displacement (PRESSS Loading History).

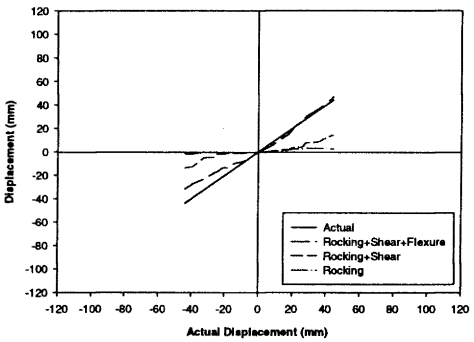

Figure 23(d) Components of Displacement (PWRI Loading History).

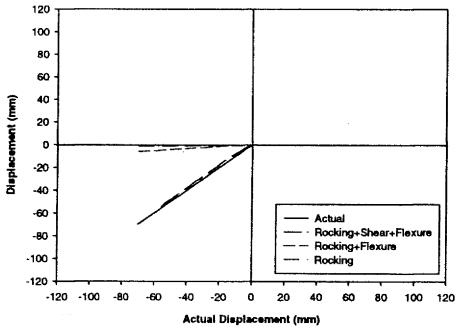

Figure 23(e) Components of Displacement (Monotonic Loading).

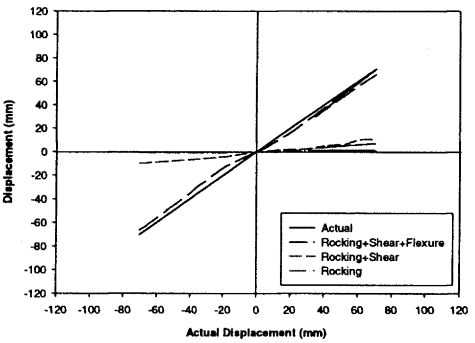

Figure 23(f) Components of Displacement (Cycling at Ductility 8).

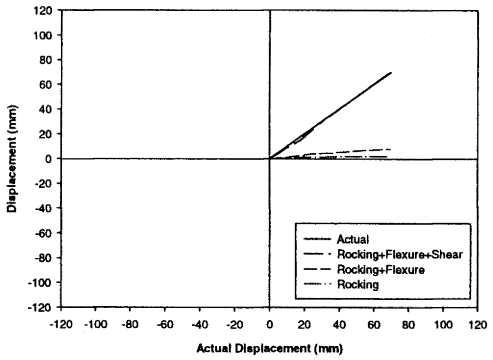

Figure 23(g) Components of Displacement (Unidirectional Loading).

referring to the two largest cracks. Table 1 was based on the maximum value measured from both sides of the test unit in both the positive and negative direction of loading. Table 1 also records the beam elongation measured at ductility 2, corresponding with the data shown in Fig. 26.

Different crack behaviour resulted from the seven different loading histories due to localised discontinuities. This effect can be seen by comparing crack widths arising during the first half cycle from bi-directional loading at ductility 8 with crack widths from monotonic loading.

Table 1 also reveals differences between the widths of cracks from the different tests. Tests where damage was more prominent after the ductility 2 cycles; such as from using the PWRI loading history, had wider cracks than tests with little damage at this loading stage, such as from the New Zealand

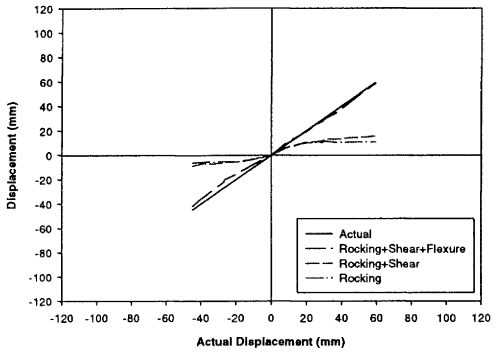

Figure 24(a) Components of Displacement (Acceleration History A).

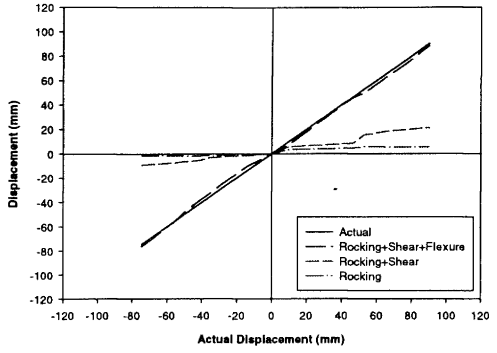

Figure 24(b) Components of Displacement (Acceleration History B).

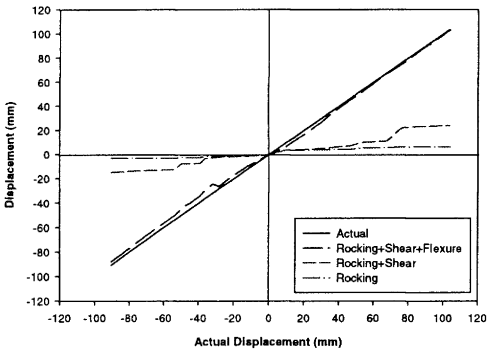

Figure 24(c) Components of Displacement (Acceleration History C).

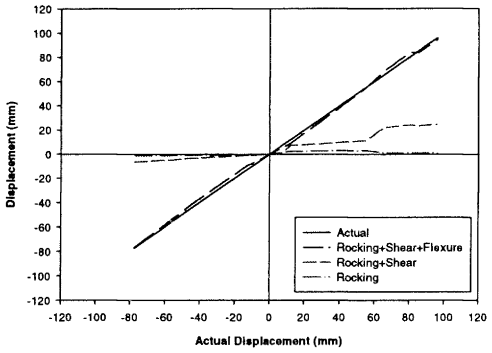

Figure 24(d) Components of Displacement (Acceleration History D).

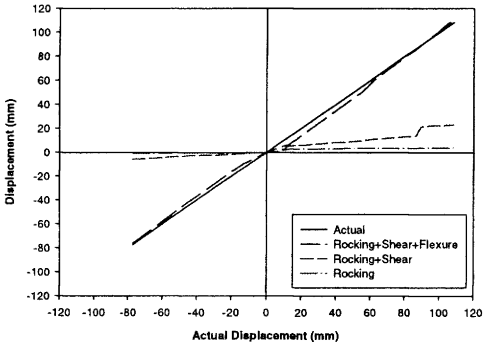

Figure 24(e) Components of Displacement (Acceleration History E).

loading history. The narrow cracks measured during testing using the UCB loading history reflected the large percentage of vertical displacement that was associated with rocking deformations (see Fig. 23(b)).

The sum of the two crack widths detailed in Table 1 generally accounted for between 50-70% of the total horizontal elongation. The exceptions to this were the crack widths measured during testing using the New Zealand and the PWRI loading histories. This was due to the width of cracks not being measured immediately next to the strain gauges. Thus, crack widths were measured that were inconsistent with the strains recorded in the gauges at the top and bottom of the beam.

4.7.2 Comparison after Loading to Ductility 4

Table 2 compares the widths of the two major cracks in the plastic hinge zone at ductility 4. Cracking from testing using the New Zealand loading history and the bi-directional cycling at ductility 8 contained more secondary cracking in the plastic hinge zone than the other tests. More testing is required to determine whether this was due to the applied loading history or the physical properties of the beam.

Table 2 reveals that varying crack widths were measured after loading to ductility 4 in each test. In general the crack widths reflected the amount of damage that had occurred in the test specimen. The exception to this was the crack widths measured when using the New Zealand loading history.

As with the response after loading at ductility 2, the sum of the two crack widths detailed in Table 3 generally accounted for between 50-70% of the total horizontal elongation. Again the exception to this was the crack widths measured during testing using the New Zealand and the PWRI loading histories.

4.7.3 Comparisons after Loading to Ductility 6

Table 3 compares the widths of the cracks from the seven tests at conclusion of the ductility 6 cycles. No additional cracking was observed for testing using the PRESSS and PWRI loading histories, and only a small amount of additional cracking was seen in the other tests. Table 3 reveals that again, the widest cracks were measured on the test specimens that had suffered the most damage.

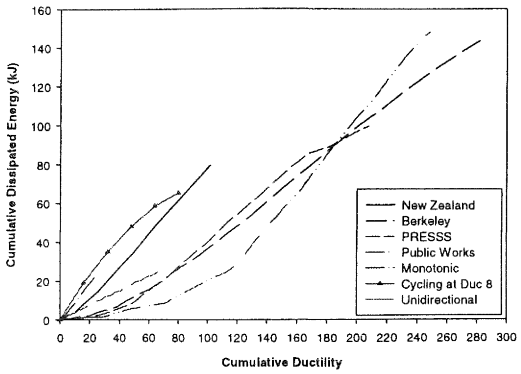

Figure 25(a) Comparison of Energy Dissipated during Laboratory Procedures

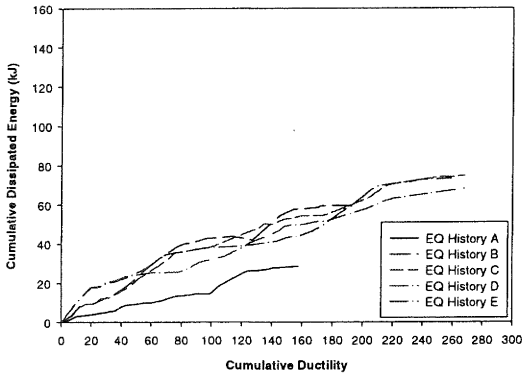

Figure 25(b) Comparison of Energy Dissipated from Acceleration Histories.

5 CONCLUSIONS

5.1 Experimental Results

Welding of instrumentation studs to the longitudinal reinforcement influenced the local material properties of the reinforcement. In some cases this lead to premature failure occurring during testing.

The ultimate displacement from monotonic and unidirectional loading was over twice the value recorded from any bi-directional cyclic tests.

Differences were noted in the ultimate displacements measured when testing using different loading histories. Testing using the PWRI loading history was the most conservative whereas testing conducted using the New Zealand loading history was the least conservative.

Variations in the applied displacement sequence for the five acceleration histories did not cause significant discrepancies in the overall response of the structure.

Failure had not occurred after the test subassemblage was subjected to four magnified earthquake records, even though two of the four records were from severe earthquakes. This indicated that structures designed using force-based methods have a high degree of conservatism inherent in their design.

The reloading stiffness and the amount of pinching in the hysteresis loops were not reliable indicators of the amount of degradation that had occurred. Instead these parameters need to be considered in conjunction with the composition of the total displacement and the energy dissipation characteristics of the displacement components.

Flexural deformations accounted for a larger percentage of the total displacement for testing using the New Zealand loading history than for testing using other laboratory procedures. This was due to the larger ductility increments that were applied in the New Zealand loading history compared to other loading histories.

Cumulative dissipated energy and cumulative ductility were not sufficiently independent of the applied loading history to be used to compare test results.

The recorded reinforcement strains at failure of the test subassemblage were found to vary, as did the measured beam elongation. Therefore, as with the amount of energy dissipated, the recorded strains in the longitudinal reinforcement cannot be used as a basis for comparison of

Table 1 Comparison of Crack Widths after Loading to Ductility 2.

Test	Crack A (mm)	Crack B (mm)	Elongation (mm)
New Zealand	1.5	0.2	1.4
Berkeley	0.3	0.2	0.9
PRESSS	1.2	1.0	3.7
Public Works Research Institute	2.2	0.4	2.3
Monotonic	1.5	0.3	2.7
Cycling at Ductility 8	1.0	0.3	2.7
Unidirectional	0.3	0.8	2.5

Table 2 Comparison of Crack Widths after Loading to Ductility 4.

Test	Crack A (mm)	Crack B (mm)	Elongation (mm)
New Zealand	5.0	0.5	5.2
Berkeley	2.8	3.2	6.8
PRESSS	2.8	4.0	11.4
Public Works Research Institute	9.0	0.5	10.7
Monotonic	3.5	0.3	6.7
Cycling at Ductility 8	3.5	0.3	7
Unidirectional	2.5	2.3	6.8

Table 3 Comparison of Crack Widths after Loading to Ductility 6.

Test	Crack A (mm)	Crack B (mm)	Elongation (mm)
New Zealand	7.5	3.5	10.4
Berkeley	5.5	6.5	17.6
PRESSS	6.0	8.0	24.2
Public Works Research Institute	-	-	-
Monotonic	5.0	0.3	10.7
Cycling at Ductility 8	4.5	2.5	11.3
Unidirectional	3.5	3.5	10.6

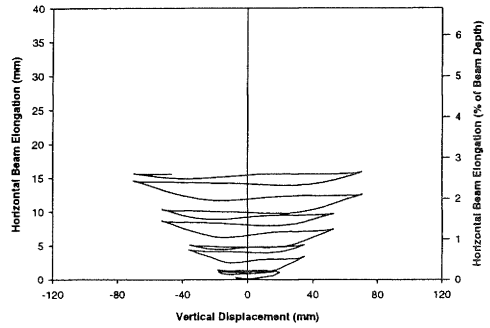

Figure 26(a) Horizontal Beam Elongation (New Zealand Loading History).

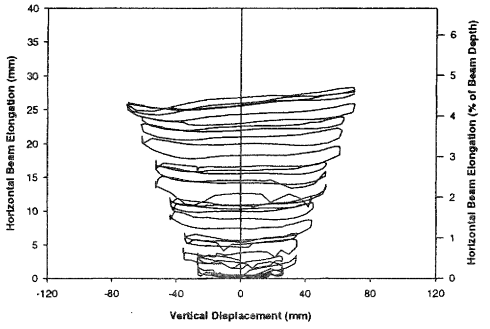

Figure 26(b) Horizontal Beam Elongation (UCB Loading History).

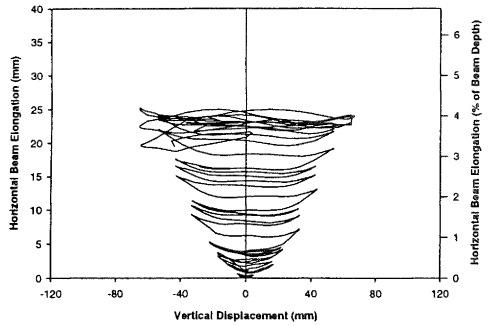

Figure 26(c) Horizontal Beam Elongation (PRESSS Loading History).

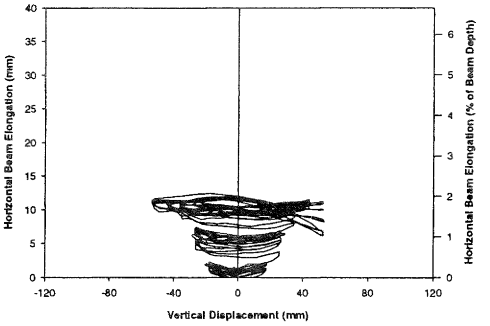

Figure 26(d) Horizontal Beam Elongation (PWRI Loading History).

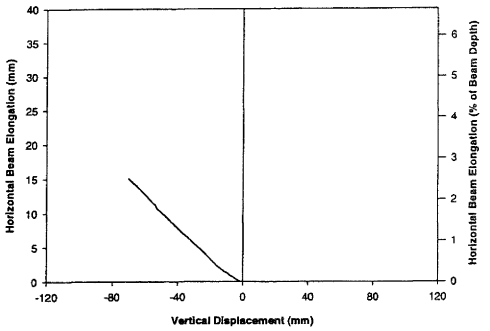

Figure 26(e) Horizontal Beam Elongation (Monotonic Loading).

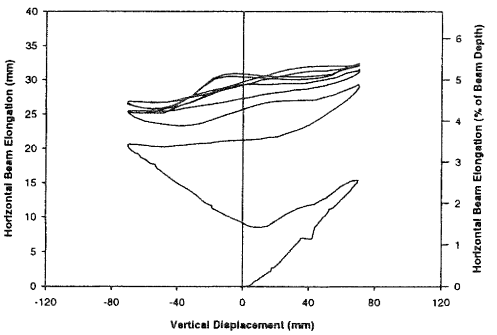

Figure 26(f) Horizontal Beam Elongation (Cycling at Ductility 8).

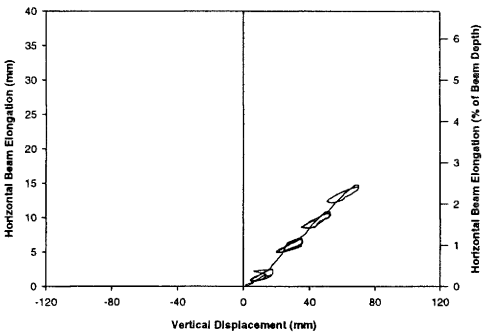

Figure 26(g) Horizontal Beam Elongation (Unidirectional Loading).

experimental results from different loading regimes.

The loading histories applied at research institutions are more demanding than actual displacements resulting from seismic excitation. However, of the loading histories from research institutions, the New Zealand loading history replicated the earthquake demand more closely than loading histories from other research institutions.

Cracking patterns are too subjective to be used as a measure of the differences between tests and crack widths only provide a general indication of the amount of damage that occurred. Cracking was also influenced by local discontinuities in the beam that were introduced during construction. However, the widths of cracks can be used during post-earthquake inspections of structures to help

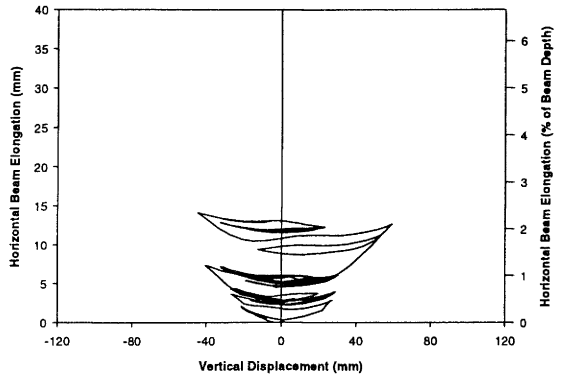

Figure 27(a) Horizontal Beam Elongation (Acceleration History A).

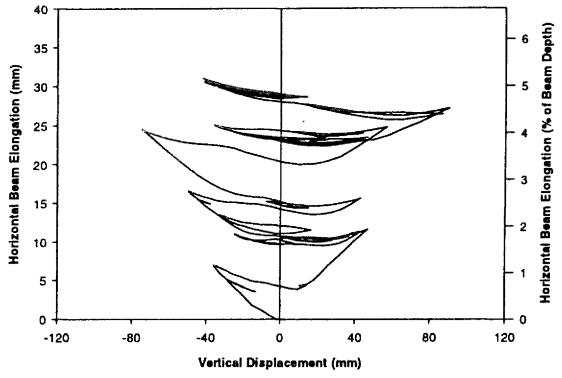

Figure 27(b) Horizontal Beam Elongation (Acceleration History B).

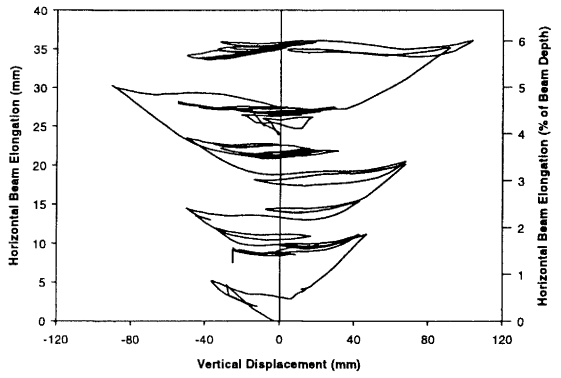

Figure 27(c) Horizontal Beam Elongation (Acceleration History C).

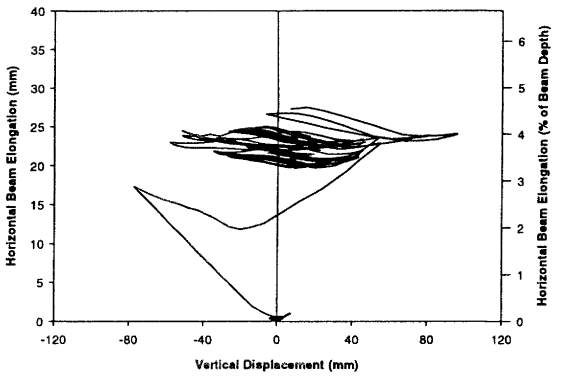

Figure 27(d) Horizontal Beam Elongation (Acceleration History D).

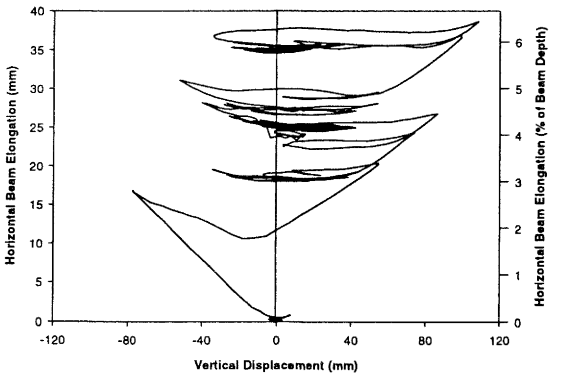

Figure 27(e) Horizontal Beam Elongation (Acceleration History E).

determine the extent of the damage, because these inspections are generally more subjective in nature.

5.2 Recommendations for Future Research

This study demonstrated that the ultimate displacement of a test subassemblage was dependent on the applied loading procedure. Therefore the international adoption of a common loading history would aid in the transfer and interpretation of research data between countries.

Welding instrumentation studs to the longitudinal reinforcement affected the experimental results. Therefore, instrumentation connections that do not result in changes to local material properties of the longitudinal reinforcement need to be investigated.

Further testing is required to investigate whether the conclusions stated herein are particular to the beam detail adopted in this study; that is, whether the results would change for different beam steel content and moment to shear ratios.

The prototype structure adopted in this study was based on a building designed to ductility 6 requirements in NZS 3101:1995. It is necessary to investigate whether comparable results would be obtained if this exercise were repeated for structures designed to a lower ductility level.

6 ACKNOWLEDGEMENTS

Hank Mooy and Mark Byrami are thanked for their assistance in building and testing the subassemblies reported herein. Thanks also to Shigeki Unjoh from the Public Works Research Institute in Japan for his help in implementing the PWRI loading history, and Sri Sritharan from Iowa State University for his help in obtaining references from the United States.

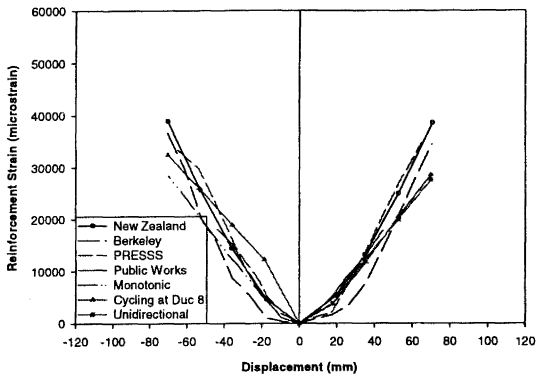

Figure 28(a) Comparison of Reinforcement Strain Envelopes for Acceleration Histories.

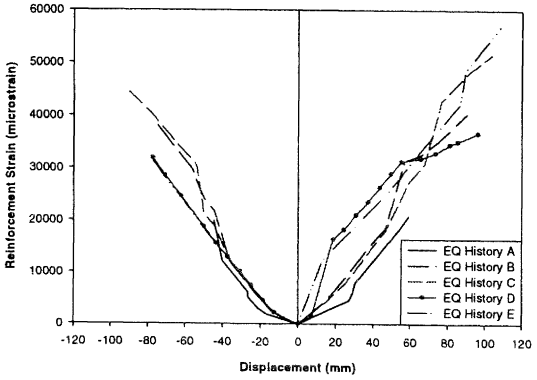

Figure 28(b) Comparison of Reinforcement Strain Envelopes for Acceleration Histories.

The Earthquake Commission Research Foundation and the Cement and Concrete Association of New Zealand provided financial support for this project. Pacific Steel Ltd and Ready Mix Concrete Ltd are thanked for donating the necessary reinforcing steel and concrete for this project. Thanks are also extended to Sika NZ Ltd for providing a place and means to build the test subassemblies and to W. Stevenson and Sons Ltd for transporting the test subassemblies to the laboratory.

7 REFERENCES

Cement and Concrete Association of New Zealand (CCANZ) (1998) "Examples of Concrete Structural Design to New Zealand Standard 3101".

Ingham, J. M. (2000) "A presentation of the PRESSS technology applied to a 39-storey building by Pankow Builders in California", New Zealand Concrete Society Conference, Wairaki, October, pp. 27-32.

Ingham, J. M., Liddell, D., and Davidson, B. J. (2001) "An Assessment of Parameters describing the Response of a Reinforced Concrete Beam", *Bulletin of the New Zealand National Society for Earthquake Engineering* (under review).

Ma, S.-Y. M., Bertero, V. V., and Popov, E. P. (1976) "Experimental and Analytical Studies on the Hysteretic Behavior of Reinforced Concrete Rectangular and T-Beams" *Earthquake Engineering Research Center*, 76-2.

Park, R. (1989) "Evaluation of Ductility of Structures and Structural Assemblages from Laboratory Testing" *Bulletin of the New Zealand National Society of Earthquake Engineering*, 22(3), pp. 155-166.

Priestley, M. J. N. (1997) "Displacement-Based Seismic Assessment of Reinforced Concrete Buildings." *Journal of Earthquake Engineering*, 1(1), pp. 157-192.

Standards New Zealand (1995) "NZS 3101:1995—New Zealand Standard for Design of Concrete Structures" 256p.

Stone, W. C., Cheok, G. S., and Stanton, J. F. (1995) "Performance of Hybrid Moment-Resisting Precast Beam-Column Concrete Connections Subjected to Cyclic Loading" *ACI Structural Journal*, 91(2), pp. 229-249.